Transmembrane Biogenesis of Kv1.3†

LiWei Tu,‡ Jing Wang,‡ Andrew Helm,‡ William R. Skach,§ and Carol Deutsch*,‡

Department of Physiology, University of Pennsylvania, Philadelphia, Pennsylvania 19104-6085, and Department of Medicine, Division of Molecular Medicine, Oregon Health Sciences University, Portland, Oregon 97201

Received July 27, 1999; Revised Manuscript Received October 20, 1999

ABSTRACT: Using a combination of protease protection, glycosylation, and carbonate extraction assays, we have characterized the topogenic determinants encoded by Kv1.3 segments that mediate translocation events during endoplasmic reticulum (ER) biogenesis. Transmembrane segments S1, S2, S3, S5, and S6 initiate translocation, only S1 and S2 strongly (>60%) anchor themselves in the membrane, S5 exhibits signal anchor activity and contains a cryptic cleavage site, and S3 and S6 fail to integrate into the membrane. Elongation of each single-transmembrane construct to include multiple transmembrane segments alters integration and translocation efficiencies, indicating that multiple topogenic determinants cooperate during Kv1.3 topogenesis and assembly. Several surprising findings emerged from these studies. First, in the presence of T1, the N-terminal recognition domain, S1 was unable to initiate either translocation or membrane integration. As a result, S2 likely functions as the initial signal sequence to establish Kv1.3 N-terminus topology. Second, S4 independently integrates into the membrane. Third, S6 plus the C-terminus of Kv1.3 is a secretory protein but can be converted to a membrane-integrated protein with a correctly oriented, cytosolic C-terminus by linking S6 to S5 and the pore loop. These results have implications for the role of the N-terminus in Kv biogenesis and on the mechanisms of dominant negative suppression of Kv1.3 by truncated Kv1.3 fragments [Tu et al. (1996) *J. Biol. Chem. 271*, 18904−18911].

Despite the precise architectural details now available for the bacterial K^+ channel, KcsA (*1*, *2*), we do not know how this, or any other, K^+ channel arrives at its final tetrameric structure. Each KcsA subunit contains only two transmembrane segments vis-à-vis the voltage-gated K^+ (Kv) channels, which contain six transmembrane segments (S1−S6) and long N- and C-termini. These general topological characteristics of Kv channels have been verified by Shih and Goldin (*3*) using a FLAG-tagged *Shaker* K^+ channel. In Kv channels, the transmembrane segments S5 and S6 and the intervening loop are highly homologous to the corresponding transmembrane segments and intervening pore region in KcsA. What is the sequence of steps by which these, and the additional Kv transmembrane segments, their intervening loops, and termini are arranged and folded to ultimately form the Kv channel with its highly evolved gating and permeation functions?

Such questions have been addressed for several other eukaryotic polytopic proteins. Topogenesis occurs cotranslationally in the erythrocyte anion transporter and the mercury-insensitive water channel, e.g., the N-terminal transmembrane segments establish topology before the translation of the C-terminus is complete (*4*, *5*). In contrast, in the cystic fibrosis transmembrane regulator, CFTR, the first transmembrane segment achieves its topology post-translationally (*6*). Interactions between topogenic determinants of polytopic proteins occur and have been demonstrated, for example, in lac permease (*7*), human P-glycoprotein (*8*, *9*), and yeast Sec61 (*10*).

In this paper, we report the results of experiments aimed at elucidating the mechanism(s) by which Kv1.3, a *Shaker*-like Kv channel, achieves its final topology in the endoplasmic reticulum (ER)[1] membrane. We have used protease protection, carbonate extraction, and N-linked glycosylation as assays for membrane topology and integration of constructs containing a C-terminal translocation reporter. These assays enabled us to identify the sequence of topogenic events mediated by each segment of the protein and the interaction, or lack thereof, between segments. Moreover, these results have some bearing on the role of the N-terminus in Kv biogenesis and on the mechanisms of dominant negative suppression of Kv1.3 by truncated Kv1.3 fragments (*11*). In the latter case, defining the transmembrane topology of these fragments is critical to understanding the relationship between suppression and physical association of the fragments with channel subunits.

MATERIALS AND METHODS

Construction of cDNA Vectors. The following primers were synthesized by the Nucleic Acid Facility of the

† Supported by National Institutes of Health Grants GM 52302 and GM 53457.

* Corresponding author: Phone 215-898-8014; Fax 215-573-5851; Email cjd@mail.med.upenn.edu.

‡ University of Pennsylvania.

§ Oregon Health Sciences University.

[1] Abbreviations: ER, endoplasmic reticulum; RRL, rabbit reticulocyte lysate; PK, proteinase K; P, C-terminus translocation reporter derived from bovine prolactin; S6C-P, S6 plus the complete C-terminus of Kv1.3; C-P, the C-terminus of Kv1.3 with a C-terminal P-reporter; Prl, secretory bovine prolactin protein; TM, a bitopic integral membrane protein, S.L.ST.gG.P; Kv1.3(T1$^-$), deletion mutant of Kv1.3 that lacks the first 141 amino acids.

10.1021/bi991740r CCC: $19.00
Published on Web 01/07/2000

University of Pennsylvania and used to make the pSP plasmids described below. The underlined sequences indicate the enzyme sites used for making fusion proteins.

antisense oligonucleotides

(1) 5′-GAGCAGGGTCACCTGGCGCTGGAAT-3′

(2) 5′-GAAAGGGGGTCACCAAGCTGGAGGCT-CCTGC-3′

(3) 5′-CATGATGGTCACCGAGAAGGTGGC-TTTGC-3′

(4) 5′-CAGGATGGTCACCCGACATGGCCTGC-TGTCC-3′

(5) 5′-TCCCAGGGTCACCATGGACGCCT-TCAGCG-3′

(6) 5′-CACAATGGTCACCCCTATGGTCACTGGG-3′

(7) 5′-AACATCGGTCACCATCTTTTTGA-TGTTGAC-3′

(SP) 5′-ATAATGGATCCTCTAGAG-3′

sense oligonucleotides

(S4) 5′-ACGACCATGGCCGAACGACAGGGC-3′

(S5) 5′-ACGACCATGGGGCAAACGCTGAAG-3′

(loop$_{5,6}$) 5′-ACTACACCATGGGTACCGAGG-CAGACGACCCCACTTC-3′

(Sp6) promoter

Clones 1−*7* (Figure 4) were constructed by PCR amplification of Kv1.3(T1$^-$) (*12*), using antisense primers 1−7, respectively, sense primer Sp6 (promoter), and ligation of the *Nco*I/*Bst*EII-digested PCR fragments into an *Nco*I/*Bst*EII-digested vector, S.L.ST.gG.P (*13*). The resulting plasmids encode regions of Kv1.3(T1$^-$) fused to a 142-residue C-terminal fragment of bovine prolactin, the so-called P-reporter (P). The S2 family P-reporter clones, S2-P, S2-S3-P, S2-S3-S4-P, and S2-S3-S4-S5-P were constructed by isolating *Ppu*mI/*Bam*HI fragments from clones 3−6, respectively, and ligating them into a *Ppum*I/*Bam*HI-digested pSP/S2-S3-S4-S5-S6COOH, which was made by religation of a *Sma*I/partially digested/*Nco*I-digested pSP/Kv1.3 plasmid. S3-S4-S5-S6C-P was constructed by religation of a *Hin*dIII/*Nru*I-digested, blunt-ended clone 7. The other S3 family clones, S3-P, S3-S4-P, S3-S4-S5-P, were constructed by religation of *Nco*I mung bean-treated/*Nru*I-digested, blunt-ended clones 4, 5, and 6, respectively. S4-P, S4-S5-P, and S4-S5-S6C-P were constructed by PCR amplification of clones 5, 6, and 7, respectively, using antisense primer SP, sense primer S4, and ligation of the *Nco*I/*Bam*HI-digested fragments into an *Nco*I/*Bam*HI-digested clone 7. S5-P and S5-S6C-P were constructed by PCR amplification of clones 6 and 7, respectively, using antisense primer SP, sense primer S5, and ligation of the *Nco*I/*Bam*HI-digested clone 7. S6C-P was constructed by religation of an *Nco*I/*Dra*III-digested, filled-in and blunt-ended, clone 7. C-P was constructed by religation of an *Nco*I/Eco72-digested, filled-in and blunt-ended, S6C-P clone. Loop$_{5,6}$-S6C-P was constructed by PCR amplification of clone 7, using antisense primer SP, sense primer loop$_{5,6}$, and ligation of an *Nco*I/*Bam*HI-digested fragment into an *Nco*I/*Bam*HI-digested clone 7. Loop$_{5,6}$-P was constructed by PCR amplification of clone 6, using antisense primer SP, sense primer loop$_{5,6}$, and ligation of an *Nco*I/*Bam*HI-digested fragment into an *Nco*I/*Bam*HI-digested clone 7. The T1-containing P-reporter clones, T1-S5-P, T1-S5-S6-P, and T1-S6C-P, were constructed by ligation of *Nco*I/*Bam*HI-digested fragments from clones S5-P, S5-S6C-P, and S6C-P, respectively, into an *Nco*I/*Bam*HI-digested pSP/Kv1.3. T1-S1-P and T1-S1-S2-P were constructed by PCR amplification of pSP/Kv1.3, using antisense primers 2 and 3, respectively, sense primer Sp6, and ligation of the *Hin*dIII/*Bst*EII-digested PCR fragments into an *Hin*dIII/*Bst*EII-digested vector S.L.ST.gG.P.

In Vitro Transcription and Translation. Capped cRNA was synthesized in vitro from linearized templates using Sp6 RNA polymerase (Promega, Madison, WI). Proteins were translated in vitro with [^{35}S]methionine (2 μL/25μL translation mixture; 10 μCi/μL, Express, Dupont NEN Research Products, Boston, MA) for 120 min at 30 °C in rabbit reticulocyte lysate, in the presence or absence of canine pancreatic microsomal membranes (2.3 μL of membrane suspension/25 μL of translation mixture) (Promega, Madison, WI) according to the Promega protocol and application guide. In time course experiments, the translation reaction was carried out at 30 °C for the indicated times up to 240 min.

Glycosylation Assays. *In vitro* translated protein (∼1−2 μL of translation mixture) was denatured in a total volume of 17 μL of denaturing buffer (0.5% SDS and 1% β-mercaptoethanol) by heating to 100 °C for 5 min. The reaction was then cooled on ice, and then 2 μL of G5 buffer (0.5 M sodium citrate) and 1−2 μL of endoglycosidase H (NEN BioLabs) were added. The reaction was incubated in a water bath at 37 °C for 1−2 h and analyzed by SDS−PAGE. N-Linked glycosylation of nascent polypeptides is mediated by membrane-bound oligosaccharyl transferase only in the ER lumen, and therefore the presence of N-linked sugars provides evidence that a particular consensus site was independently translocated.

Protease Digestion. Proteinase K (PK) was added to the translation mixture to a final concentration of 0.2 mg/mL in the presence or absence of 1% Triton X-100, incubated on ice for 1 h, and inactivated with phenylmethanesulfonyl fluoride (PMSF; 10 mM), followed by SDS−PAGE. For immunoprecipitation experiments, PMSF-inactivated samples were immunoprecipitated with anti-prolactin antibody (ICN, Costa Mesa, CA) and analyzed by SDS−PAGE. If the C-terminus P-reporter of a protein is in the cystosol, then the P-reporter will be susceptible to proteolytic digestion and the protein will not be immunoprecipitated. In contrast, if the C-terminus P-reporter resides in the lumen, then the P-reporter will be protected in the absence of detergent and the protein can be recovered by immunoprecipitation. To test for protection efficiency, the fully secretory protein bovine prolactin (Prl) was examined. The percentage of Prl protected from protease digestion was typically ∼90%. The percentage of P-reporter protection for other constructs was calculated as the ratio of the counts per minute (cpm) for PK-protected fragments relative to the cpm for the parent P-reporter construct, corrected for proteolytic loss of methionine in each fragment, which was estimated by size (molecular weight) of the protected fragment and location of methionines relative to cleavage sites. Where multiple protected fragments were

generated, the maximum percent P-protection for each construct was calculated as the percent P-protection of the full-length P-reporter parent plus the contribution of all recovered P-reactive fragments derived from the parent during PK digestion.

Immunoprecipitation and Autoradiography. PK-digested products (7 μL, PMSF-inactivated) were diluted into 1 mL of buffer A [0.1 M NaCl, 0.1 M Tris (pH 8.0), 10 mM EDTA, and 1% Triton X-100] containing 1 mM PMSF, and mixed with 0.5 μL of anti-prolactin antiserum (ICN Biomedicals, Costa Mesa, CA) and incubated at 4 °C for 30−60 min. Protein A Affi-Gel beads (10 μL, Bio-Rad, Hercules, CA) were added, and the sample was continuously mixed at 4 °C for 2−10 h prior to washing 3× with Buffer A and twice with 0.1 M NaCl, 0.1 M Tris, pH 8.0. Samples were analyzed by SDS−PAGE. Electrophoresis was performed on a C.B.S. Scientific gel apparatus using SDS−12.5% polyacrylamide gels made according to standard Sigma protocols (Sigma Technical Bulletin, MWM-100). Gels were soaked in Amplify (Amersham Corp., Arlington Heights, IL) to enhance ^{35}S fluorography, dried, and exposed to Kodak X-AR film at −70 °C. Typical exposure times were <36 h. Gels were quantitated directly with a Molecular Dynamics PhosphoImager (Sunnyvale, CA).

Carbonate Extraction. A carbonate extraction assay was used to distinguish between lumenal/peripheral and integral membrane proteins (*14*). In vitro translation products (0.5−1.0 μL) were diluted in 750 μL of either sodium carbonate (0.1 M Na_2CO_3, pH 11.5) or Tris (0.25 M sucrose and 0.1 M Tris, pH 7.5) solution, incubated on ice for 30 min, and centrifuged at 70 000 rpm (208 kG) TLA 100.3 rotor for 30 min. Supernatants were removed, precipitated with 10% trichloroacetic acid, and resuspended in 20−40 μL of SDS−PAGE sample buffer. Membrane pellets were dissolved directly in SDS−PAGE sample buffer. Under these conditions, lumenal and peripheral proteins are extracted at pH 11.5 (supernatant), whereas integral membrane proteins remain membrane-associated (pellet) (*14*).

Transmembrane and secretory control proteins were S.L.ST.gG.P and bovine preprolactin, respectively. The former (referred to as TM in Figures 2 and 7), encodes a chimeric integral transmembrane protein of 45 kDa (*13*) and the latter encodes a secretory protein (Prl, 25 kDa). As expected, for Prl, the ratio $\{\text{pellet}/(\text{pellet} + \text{supernatant})\}_{\text{Tris}}$ in Tris buffer was always >90%. This reflects the high efficiency of microsomal targeting and translocation and integrity of the microsomal membrane. Recovery of Prl protein in carbonate buffer was assessed as the ratio of $\{\text{supernatant}/(\text{pellet} + \text{supernatant})\}_{\text{carbonate}}$ and was always ∼90%. To ensure that membrane concentration was not limiting, membranes were added in sufficient concentration to keep the percent of total signal in the Tris supernatant <10% for both control proteins. This was also true for all Kv1.3 constructs except S4-P, C-P, $\text{loop}_{5,6}$, T1-S1, T1-S1-P, and T1-S6C-P. The percent of protein [$(SX)_n$-P] integrated into the membrane was calculated as {pellet cpm in carbonate/(pellet cpm in carbonate + corrected supernatant in carbonate)}. The supernatant correction factor was 1.1−1.2 for all experiments, reflecting the 80−90% recovery of Prl in the carbonate supernatant. Integration efficiency for membrane integrated protein was assessed as the ratio for S.L.ST.gG.P of $\{\text{pellet}_{\text{carbonate}}/(\text{pellet} + \text{supernatant})_{\text{Tris}}\}$ The integration efficiency was ∼90%.

Oocyte Electrophysiology. Oocytes were isolated from *Xenopus laevis* females (Xenopus I, Michigan) as described previously (*15*). Stage V−VI oocytes were selected and microinjected with 1−2 ng of cRNA encoding Kv1.3. K^+ currents from cRNA-injected oocytes were measured with two-microelectrode voltage-clamp using a OC-725C oocyte clamp (Warner Instrument Corp., Hamden, CT) after 15−72 h, at which time currents were >2 μA. Electrodes (<1MΩ) contained 3 M KCl. The currents were filtered at 1 kHz. The bath Ringer solution contained 116 mM NaCl, 2 mM KCl, 1.8 mM $CaCl_2$, 2 mM $MgCl_2$, and 5 mM Hepes (pH 7.6). The holding potential was −100 mV. For suppression experiments, data are presented as box plots, which represent the central tendency of the measured current. The box and the bars indicate 25−75th and 10−90th percentile of the data, respectively. The horizontal line inside each box represents the median of the data.

RESULTS

Topogenic Determinants of Individual Transmembrane Segments of Kv1.3. To elucidate the mechanisms by which a Kv channel achieves its final topology, we determined the ability of each transmembrane segment to initiate and terminate translocation across the microsomal membrane and to integrate into the membrane with a specific orientation. We generated a series of constructs containing a C-terminus translocation reporter (P) derived from bovine prolactin (*13*, *16*). Protease protection assays, as described below, were used to determine whether the C-terminus reporter resided in the cytosol (susceptible to protease digestion) or in the lumen of the microsomal membrane vesicle (protected from protease digestion). Because N-linked glycosylation occurs only in the ER lumen (*17*), detection of glycosylation was used to assess translocation of consensus glycosylation sites. Finally, carbonate extraction was used to distinguish between lumenal/peripheral polypeptides and integral membrane proteins (*14*). These approaches have been used similarly to localize topogenic transmembrane sequences in polytopic proteins (e.g., refs *8* and *18*−*20*).

The P-reporter used to examine the ability of specific transmembrane segments to initiate translocation (signal sequence activity) consists of the C-terminal 142 amino acids of bovine prolactin and contains no intrinsic topogenic information (*13*, *16*). Figure 1A illustrates the location of methionines in native Kv1.3, and Figure 1B shows the Kv1.3 sequences in the constructs S*x*-P, where *x* refers to the number (1−6) of the individual transmembrane segment. Each construct was translated in rabbit reticulocyte lysate (RRL) in the presence of microsomal membrane vesicles, treated with proteinase K (PK; Boehringer Mannheim, Germany) in the presence or absence of detergent, and then immunoprecipitated with anti-prolactin antibody and analyzed by SDS−PAGE (Figure 1C). Because PK exhibits a very broad cleavage specificity, it will cleave any part of a protein that is present and accessible in the cytosol. Relatively strong protection was observed for S1, S3, S5, and S6 (lanes 2, 8, 14, and 17), indicating that these transmembrane segments functioned as signal sequences and translocated the C-terminal P-reporter into the ER lumen. In contrast, for S2 and S4, the P-reporter was in the cytosol. S1, S2, and S6

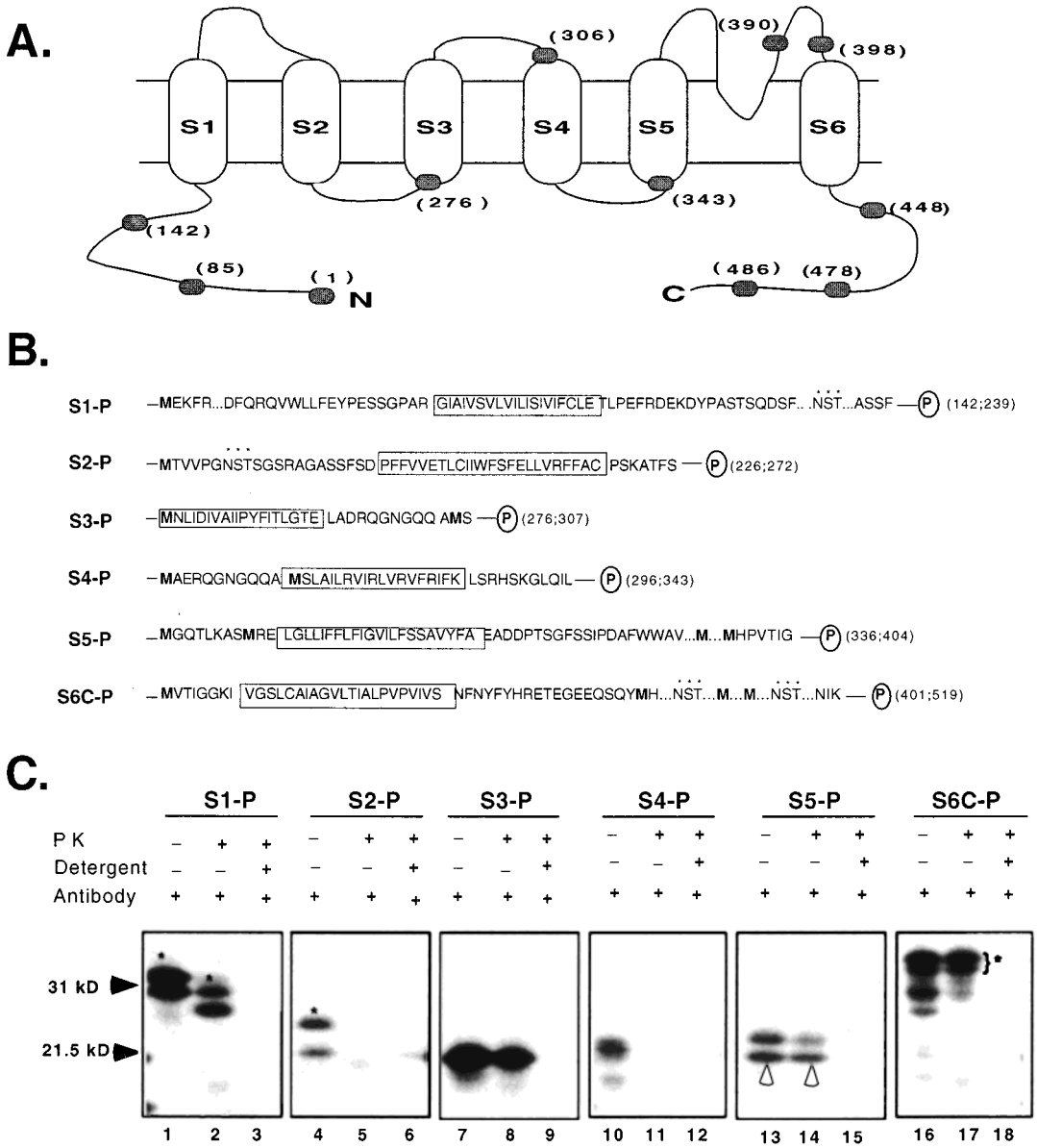

FIGURE 1: Protease digestion of S*x*-P constructs. (A) Schematic of Kv1.3 indicating the native methionines (shaded ovals). The numbers in parentheses indicate the amino acid number in the native sequence that encodes the indicated methionine. (B) Schematic of P-reporter constructs of single (S*x*-P) segments. S6 plus the complete C-terminus, including a P-reporter at the end, is denoted as S6C-P. The amino acid sequence is indicated by single-letter code and the predicted transmembrane segments are enclosed within a box. Long stretches of amino acids are indicated by ellipses (...). The numbers in parentheses are the amino acid numbers in the native sequence that encode the start and P-reporter sites, respectively. In the case of S2-P, five amino acids were inserted before the glycosylation site at amino acid 226. Methionines are indicated by **M** and the P-reporter by a boldface **P** inside an oval. (C) For the constructs shown in panel B, microsomal membranes containing translated protein were pelleted, resuspended, and incubated with proteinase K (PK) in the presence or absence of detergent as described under Materials and Methods, then immunoprecipitated with anti-prolactin antibody and analyzed by SDS−PAGE. The observed molecular mass for unglycosylated (S*x*-P) constructs are (in kilodaltons): S1-P, 29; S2-P, 21; S3-P, 20; S4-P, 21; S5-P, 23; and S6C-P, 28. A single asterisk marks a band due to glycosylated protein. Constructs S1-P and S2-P each show one additional band, and S6C-P, two additional bands (see Figure 9), due to glycosylated protein. The lower molecular weight S5-P band marked by an open, upward arrowhead is due to a signal cleavage peptidase site in S5-P.

P-reporter constructs each produced glycosylated polypeptides (bands marked by asterisks). Consensus glycosylation sites are present in the C-terminus of S1, the N-terminus of S2, and the C-terminus of S6C, thus indicating that these terminal regions of S1, S2, and S6C resided in the lumen. Glycosylation was confirmed by endoglycosidase digestion (see below). The cytosolic region of S1-P was digested by PK to give a doublet that was ~2 kDa lower than the undigested parent S1-P (lanes 1 and 2), indicating that S1 spans the bilayer. Two translation products were detected for S5-P, both of which produced P-protected proteins. The 23-kDa fragment is the correct predicted molecular weight of S5-P and was observed in the absence of microsomal membranes (data not shown). This suggests that the lower molecular weight band (Δ) arose from an internal cleavage event, presumably due to recognition of a cryptic signal peptidase cleavage site unmasked by the fusion protein. This phenomenon is frequently observed in other polytopic proteins when downstream and/or upstream transmembrane segments are removed (*20*−*23*). This interpretation was confirmed by carbonate extraction (see below). Although this site is not cleaved during normal Kv1.3 biogenesis, such a

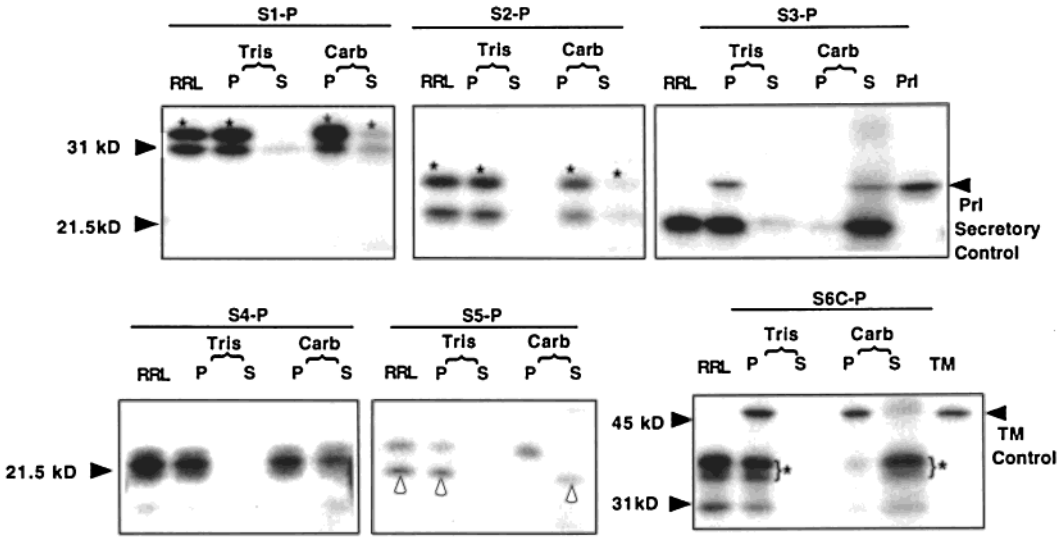

FIGURE 2: Integration into microsomal membranes of single-transmembrane constructs. The translation products (RRL lane) were extracted into either Tris buffer (pH 7.5) (Tris lanes) or carbonate buffer (pH 11.5) (carb lanes), centrifuged to give pellet (P) and supernatant (S) fractions, and analyzed by SDS−PAGE. The pellet contains the membrane fraction of protein. The following control cRNA were simultaneously translated in the assay: S.L.ST.gG.P [referred to as TM (transmembrane) in the figure], which encodes a chimeric integral transmembrane protein (45 kD) (*13*), and Prl, which encodes a secreted full-length protein (25 kD). The former should remain in the pellet fraction at pH 7.5 and pH 11.5, whereas the latter will be in the pellet (microsome lumen) at pH 7.5 and in the supernatant at pH 11.5. A single asterisk marks a band due to glycosylated protein; filled, sideways arrowheads mark control protein bands, Prl or TM, and the positions of molecular mass standards. The lower molecular mass S5-P band marked by an arrowhead is due to a signal cleavage peptidase site in S5-P.

	S1-P	S2-P	S3-P	S4-P	S5-P	S6C-P
% Integration	85%	67%	11%	51%	47%	17%
% P- Protection	45.3%	<10%	53.5%	<10%	62%	78%

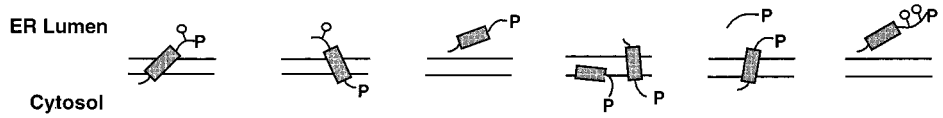

FIGURE 3: Compartment localization and orientation. A cartoon representation of compartment localization and orientation of the major species is indicated for each S*x*-P construct. The shaded rectangles represent transmembrane segments and the ball-and-stick represents a glycosylated residue. The percent integration and P-protection were calculated, as described under Materials and Methods, for data shown in Figures 1 and 2. The percent protection for S1-P is corrected for loss of one out of five methionines due to PK digestion (i.e., multiplied by 1.25). For all other constructs, the correction due to loss of methionine is <10%. The percent protection is the average of two independent experiments.

cleavage site could be used for editing purposes to limit misfolded proteins should the site become accessible or inappropriately directed to the lumen.

To distinguish whether a P-protected construct is stably anchored in the membrane with its C-terminus P-reporter in the lumen (cytosol) from one that is entirely in the lumen (cytosol), we performed carbonate extraction assays for each S*x*-P construct. Translation products were incubated in either Tris buffer (pH 7.5) or carbonate buffer (pH 11.5), and membranes were pelleted by centrifugation to give the results shown in Figure 2. The bitopic integral membrane protein S.L.ST.gG.P [45 kDa (*13*); referred to as TM in Figure 2] and the secretory protein bovine prolactin (Prl, 25 kDa), served as controls. Our results demonstrate that S1, S2, S4, and S5 integrated strongly (50−85%), whereas S3 and S6-C did not (<20%). Thus, S2 clearly spans the membrane because it was integrated and the N-terminus was in the lumen (glycosylation) while the C-terminus was in the cytosol (PK digestion). Carbonate extraction of S5-P demonstrated that the 23-kDa product was integrated into the membrane while the smaller fragment was 80% extracted like the secretory control. These results support an interpretation that the lower molecular weight band was generated from an internal cleavage event, which removed the transmembrane segment. Furthermore, we examined another S5-P construct that lacked the first eight amino acids and therefore contained only one N-terminal ATG codon. Similar results were obtained (data not shown), indicating that the lower molecular weight band was not generated from an internal ATG start codon.

The results of the protease protection assays, the carbonate extraction assays, and glycosylation for all of the single-transmembrane constructs are given in Figure 3, along with compartment distributions and orientations for the majority of the protein derived from each single-transmembrane construct. These representations reflect that S1 and S2 are strong signal anchors, while S3 and S6 lack a stop signal and behave like secretory proteins. S4 fails to translocate its C-terminus. S5 exhibits signal anchor activity and contains a cryptic cleavage site.

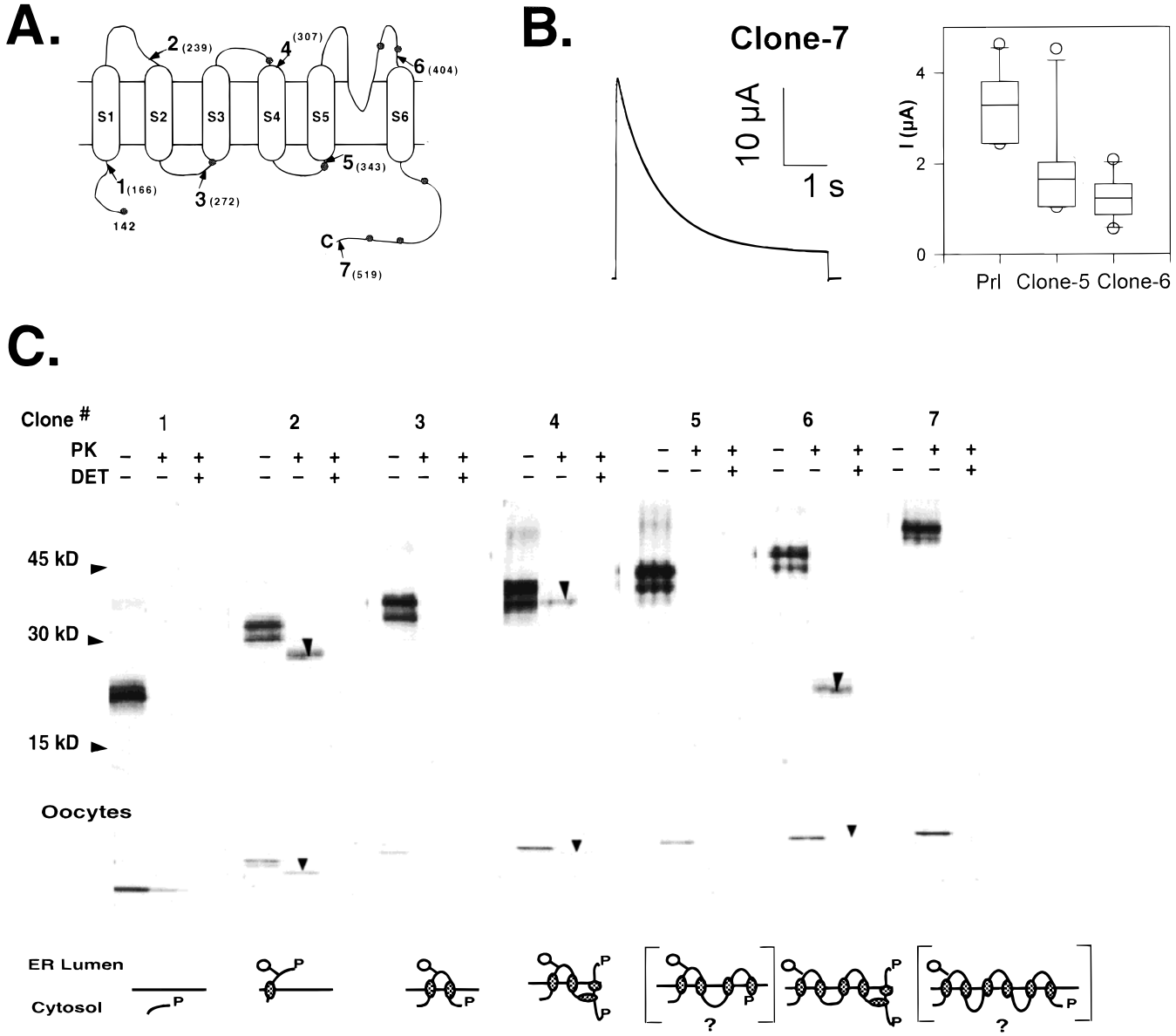

FIGURE 4: Topology of Kv1.3(T1$^-$) clones 1−7 in microsomal membranes. (A) Schematic of P-reporter constructs: clones 1−7. Boldface numbers and arrows indicate the C-terminal site at which a P-reporter was inserted to make clones 1−7. The small numbers in parentheses are the amino acid numbers in Kv1.3 that encode the P-reporter sites. Methionines are indicated by small, shaded circles. (B) *Xenopus* oocytes were injected with cRNA for clone 7 containing the P-reporter and recordings were made 24 h postinjection. Peak current at +50 mV was measured to give the current trace shown on the left. The inactivation time constant was similar to that of wild-type Kv1.3 (*11*). Suppression experiments were performed by coinjecting cRNA for Kv1.3(T1$^-$) and either Prl, clone 5, or clone 6 (in a 1:2 mole ratio) and recording peak current at +50 mV after 24 h. Data are represented as box plots ($n = 6$). The median current obtained with clones 5 and 6 were significantly less than control Prl ($p = 0.04$ and 0.002, respectively, as determined from a nonparametric Mann−Whiney rank sum test). The bath Ringer solution contained 116 mM NaCl, 2 mM KCl, 1.8 mM $CaCl_2$, 2 mM $MgCl_2$, and 5 mM Hepes (pH 7.6). The holding potential was −100 mV. (C) For the Kv1.3(T1$^-$) constructs shown in panel A, microsomal membranes containing translated protein were pelleted, resuspended, and subjected to protease incubation, immunoprecipitated with anti-prolactin antibody, and analyzed by SDS−PAGE. All translation lanes (first of three lanes for each clone), except for clone 1, display two bands for the parent, which represent glycosylated protein due to the presence of a glycosylation consensus site in the loop between S1 and S2. For parent proteins with longer chains (higher molecular weight), these bands cannot be easily resolved. The downward arrowheads indicate a P-protected protein. The panel labeled "oocytes" was derived from the expression of clones 1−7 in oocytes, subsequent isolation of ER membrane vesicles, and PK digestion, as described above for the analogous in vitro experiment. A cartoon representation of the topology is shown below each set of lanes for each construct. The shaded area represents the transmembrane segments and the ball-and-stick represents a glycosylated residue. For clone 6, the in vitro data display a P-protected 23 kDa band, whereas in oocytes, the P-protected fragment is at the molecular weight of the parent clone. These results suggest that the loop between S4 and S5 is more accessible in vitro than in vivo.

Kv1.3 Cotranslational Events. Having defined the topogenic determinants of each transmembrane segment, we compared these results to the sequence of translocation events that give rise to Kv1.3 transmembrane topology. For this purpose, we generated a series of fusion proteins in which each transmembrane segment was used sequentially to make the series of P-reporter constructs shown in Figure 4A. When possible, these proteins were tested electrophysiologically to confirm that the P-reporter did not alter function. Clone 7, which is identical to Kv1.3(T1$^-$) (*11*) but contains the additional C-terminal P-reporter, was expressed in *Xenopus* oocytes and tested for channel activity. Figure 4B shows that

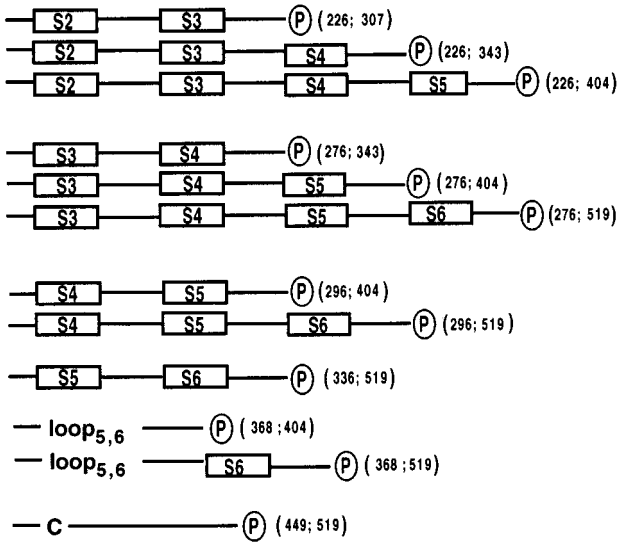

FIGURE 5: Schematic diagram of P-reporter constructs of multiple $(Sx)_n$-P transmembrane segments. The numbers in parentheses are the amino acid numbers in the native sequence that encode the start and P-reporter sites, respectively. $Loop_{5,6}$ is the loop between transmembrane segments S5 and S6 in Kv1.3.

this construct expressed current at +50 mV that inactivated with a time constant of 810 ± 83 ms ($n = 4$), similar to that produced by Kv1.3($T1^-$) (*11*). Moreover, the function of fragments of Kv1.3($T1^-$) linked to a P-reporter was tested by using the ability of such fragments to suppress current (*11*). Clones 5 and 6 suppressed current 50% (Figure 4B), similar to Kv1.3 fragments that lack a P-reporter. The results of protease protection assays of clones 1−7 are shown in Figure 4C. To confirm these in vitro findings, we expressed each of these clones in oocytes and obtained similar results (bottom panel in Figure 4C). The topological interpretation of these experiments is indicated below each construct. The topological behaviors of S2-P and S4-P in S1-S2-P and S1-S2-S3-S4-P (clones 3 and 5), respectively, were similar to the behaviors of S2-P and S4-P alone (Figure 1). In contrast, the P-protection for S3-P, S5-P, and S6-P in clones 4, 6, and 7, respectively, differed from the P-protection for S3-P, S5-P, and S6-P alone. S3-P and S5-P in clones 4 and 6 displayed weaker signal sequence activity. When the P-reporter followed S6 in clone 7, the P-reporter was in the cytosol, whereas the P-reporter following S6 in S6C-P was in the lumen. These results suggest that the presence of upstream residues is critical for properly modifying S6 topology. Likewise, upstream residues (e.g., S1, S2, and S1−S4, respectively) seem to play a role in decreasing the independent signal sequence activity exhibited by S3 and S5.

Topogenic Determinants of Multiple Transmembrane Segments. To dissect the interactions giving rise to Kv1.3 topology, we investigated the interdependence of topogenic determinants in modular units of transmembrane segments. Each single-transmembrane construct was expanded to include multiple, contiguous transmembrane segments in which the P-reporter was placed at the C-terminus of successively longer chains, as diagrammed in Figure 5. The construct C-P denotes the C-terminus of Kv1.3 with a C-terminal P-reporter. We compared protease protection of the P-reporter for these constructs to determine the influence of preceding transmembrane segments on translocation activities of transmembrane segments. As shown in Figure 6, constructs terminating with S5-P that contained multiple transmembrane segments were less protected than the single-transmembrane construct S5-P (62%, Figures 1C and 3), respectively. The maximum protection (see Materials and Methods) for S4-S5-P, S3-S4-S5-P, and S2-S3-S4-S5-P was 29%, 20%, and 48%, respectively. Elongation of S3-P and S5-P altered their ability to translocate the P-reporter, which may indicate interactions between consecutive transmembrane segments (see Discussion). Transmembrane interactions, for example between S2-S3-S4, may be manifest as an altered protein conformation. Finally, S5-S6C-P was unprotected, in contrast to S6C-P itself, which was almost fully protected, suggesting that the presence of S5 restricts the C-terminus of S6 to the cytosol. Additional evidence that S6 translocation specificity is modified by upstream residues is given by the results of glycosylation assays (see Figure 9 and Discussion).

Having defined the topology and orientation of consecutive transmembrane segments, we next determined membrane integration by carbonate extraction (Figure 7). The integration efficiency increased with increasing number of transmembrane segments for all transmembrane constructs. This was especially marked for the S3-derived constructs, where S3 alone was unable to integrate (11%), but S3-S4 and S3-S4-S5 were integrated 62% and 86%, respectively. Although each single-transmembrane segment integrated with different efficiency, all families converged to the same maximal level of integration, approximately 90%. C-P contains no transmembrane segments and it does not integrate (Figure 7A).

To determine whether the measured percent membrane integration represents a difference in kinetics or a difference in steady-state integration, we studied the time dependence of integration for constructs S1-P, S4-P, S1-S2-P, and S3-S4-P. As shown in Figure 8, by 20 min, all constructs except S4-P integrated to ~90% of their final steady-state levels. S4-P was only 26% integrated at 20 min and continued to integrate over the next 240 min to 56%, thus indicating that S4-P was slower and less efficient.

Both translocation and integration of constructs containing multiple transmembrane segments reflect interactions between topogenic determinants. This is most strikingly apparent for S6. The C-terminus of S6C-P, which has two N-linked glycosylation consensus sites, was completely translocated across the membrane. However, this region was not translocated in S5-S6C-P, similar to the behavior of the C-terminus in Kv1.3 clone 7 (Figure 4). This modification of P-reporter translocation was confirmed by glycosylation measurements of constructs C-P, S6C-P, S5-S6C-P, S4-S5-S6C-P, and S3-S4-S5-S6C-P. Each was translated in the presence or absence of microsomal membranes, and subsequently treated with endoglycosidase. As shown in Figure 9, C-P was not glycosylated, S6C-P was 80% glycosylated, and S5-S6C-P was only 15% glycosylated. Although the constructs containing multiple transmembrane segments integrate efficiently (Figure 7), they achieve only ~20% glycosylation (Figure 9B). The construct S5-S6C-P contains the pore loop ($loop_{5,6}$) between S5 and S6. To dissect the upstream element responsible for altering the topology of S6C-P in S5-S6C-P, we deleted S5 and tested whether the remaining $loop_{5,6}$ was sufficient to retain the C-terminus in the same orientation as in S5-S6C-P. As shown in Figure

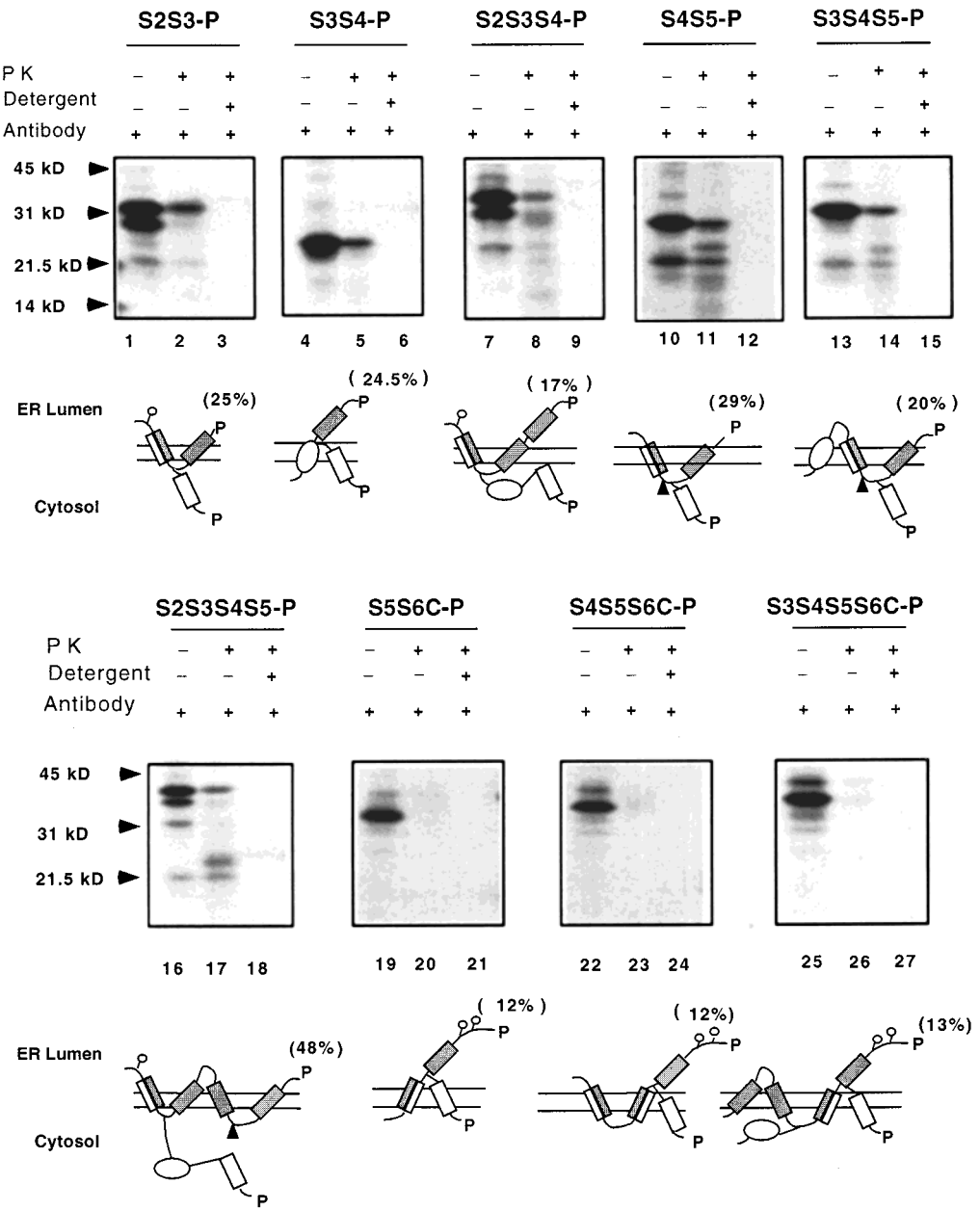

FIGURE 6: Protease protection of multiple transmembrane $(Sx)_n$-P constructs. For the constructs shown in Figure 5, microsomal membranes containing translated protein were treated as described in Figure 1 and analyzed by SDS−PAGE. Cartoon representations of the protected and unprotected orientations of each parent construct containing the P-reporter are indicated below the corresponding lanes for each $(Sx)_n$-P construct. The shaded rectangles represent the transmembrane segments belonging to the protected parent construct; the open rectangles represent the transmembrane segments belonging to the unprotected parent construct. A half-shaded, half-empty rectangle represents a transmembrane segment that is identically oriented in both the protected and unprotected parent. An oval represents intervening transmembrane segments whose topology cannot be determined in this construct. Potential proteolytic cleavage sites are indicated by filled, upward triangles. The ball-and-stick represents a glycosylated residue. The maximum percent protection is given in parentheses and was calculated as described under Materials and Methods and is the average of two independent experiments. The percent of unprotected parent constructs cannot be accurately determined and is >50% for all the constructs shown. The major species present in all these cases is the unprotected parent construct. For some constructs, minor bands may be due to incomplete translation products or internal ATG start sites.

9C, $loop_{5,6}$-P was not integrated, appearing almost quantitatively in the Tris and carbonate supernatants, and was digested >90% by PK. This construct was therefore in the cytosol. $Loop_{5,6}$-S6C-P was only 15% integrated, mostly unglycosylated (>80%), and the unglycosylated fraction was completely digested by PK, whereas the minor glycosylated fraction was protected, as revealed by longer audioradiographic detection (not shown). These results demonstrate that residues within the pore loop alter translocation specificity but not integration of S6 and suggest that S5 ensures the integration of S6C-P with the correct topology found in Kv1.3. The pore loop in $loop_{5,6}$-S6C-P provides S6 N-terminal flanking residues, which may serve to establish S6 topology (*24*).

Role of the N-Terminus of Kv1.3 in Modulating Topogenesis. Kv subfamilies contain a highly conserved cytosolic N-terminus that constitutes a subfamily specific recognition domain (*25*−*27*). Shen and Pfaffinger (*28*) defined three regions of the N-terminus, A, B, and C, and identified regions A and B as the critical recognition domain involved in intersubunit association. Regions A and B were therefore designated the "T1 domain" ["first tetramerization" domain

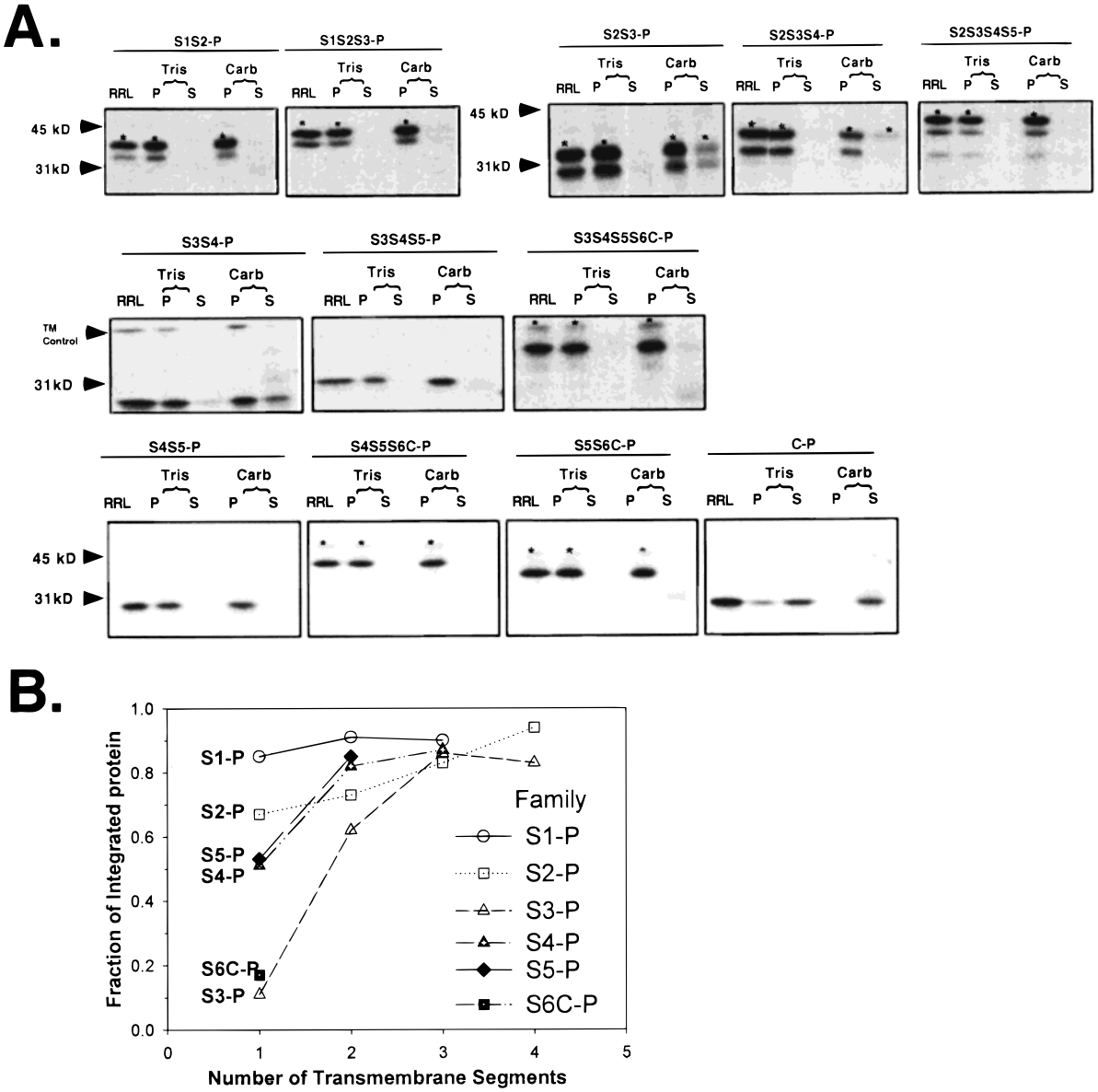

FIGURE 7: Dependence of membrane integration on number of transmembrane segments. (A) The translation products for constructs shown in Figure 5 and for S1-S2-P and S1-S2-S3-P (clones 2 and 3, Figure 4) were extracted into either Tris buffer (pH 7.5) or carbonate buffer (pH 11.5), centrifuged to give pellet (P) and supernatant (S) fractions, and analyzed by SDS−PAGE. For some constructs, incomplete translation products were present, e.g., S2-S3-S4-S5-P, lowest band. Filled, sideways arrowheads mark control protein bands, TM, and the positions of molecular mass standards. (B) Calculated fraction of protein integrated into the membrane (see Materials and Methods) for the data shown in panel A and for the data shown in Figure 2. A family of constructs is defined as the starting transmembrane segment, e.g., the S1 family includes S1-P, S1-S2-P, and S1-S2-S3-P. Each symbol represents all members of the indicated family.

(*26*)]. In Kv1.3, T1 includes residues 1−141 and S1-containing constructs start with residue 142 (i.e., region C). We have previously demonstrated that a Kv1.3 fragment containing the entire amino terminus (regions A, B, and C) plus S1 could potently and specifically suppress function of Kv1.3 (*29*). We therefore wished to know the transmembrane localization and topology of this fragment. Surprisingly, T1-S1-P, which contains the complete amino terminus (A, B, and C), was unable to initiate either translocation or membrane integration (Figure 10B, lanes 7−10). This was in marked contrast to S1-P (region C only), which directed translocation as well as integration (lanes 2−5). Similar results were obtained for T1-S1 lacking the P-reporter, both in vitro and in oocytes (data not shown). These results indicate, therefore, that the T1 domain strongly inhibits S1 signal sequence activity and suggests that other regions of Kv1.3 confer topogenic activities required to achieve the final topology of S1. This hypothesis is supported by the results shown in Figure 10B (lanes 12−15), which demonstrate that addition of S2 leads to proper translocation, glycosylation, and membrane integration of T1-S1-S2-P.

To determine whether T1 can nonspecifically inhibit the activity of any other signal sequences, we examined constructs T1-S6C-P, T1-S5-P, and T1-S5-S6C-P, respectively. As shown in Figure 11, T1-S6C-P was neither glycosylated nor integrated (only 4% integration) and was mostly in the Tris supernatant, indicating that T1 was able to prevent translocation of S6C-P. In contrast, T1 did not qualitatively alter the ability of S5-P to integrate into the membrane nor the behavior of S5-S6C-P [15% glycosylation (Figure 9B) and 85% integration (Figure 7B)]. However, a quantitative change in the behavior of T1-S5-P was significant. The

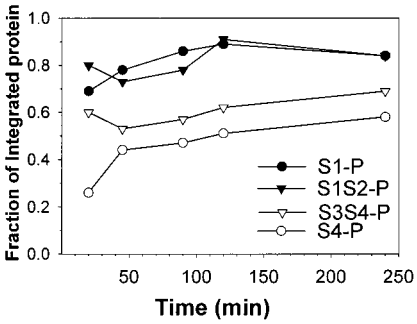

FIGURE 8: Time course of integration. At the indicated translation times, S1-P and S4-P (● and ○, respectively) or S1-S2-P and S3-S4-P (▼ and ▽, respectively) translation products were extracted into either Tris buffer (pH 7.5) or carbonate buffer (pH 11.5) and processed as described in Figure 2 to determine pellet−supernatant distributions of the protein. The fraction of membrane-integrated protein was calculated as described under Materials and Methods.

increased integration of 82% for T1-S5-P compared to 47% for S5-P (Figure 4) may indicate that the presence of T1 inhibits S5-P translocation of its N-terminus into the lumen, thereby increasing the T1-S5-P anchored in the membrane. Since T1-S5-P was targeted to the membrane (82% integration), the single translation product for T1-S5-P indicates that the cryptic S5 cleavage site in T1-S5-P was not cleaved, either because the cleavage site did not enter the lumen or because T1 masked the cryptic cleavage site. The former is more likely for the following reason. PK-digestion of T1-S5-P, shown in Figure 11C, generated two protected P-reporter fragments: an approximately 23-kDa fragment and an approximately 36-kDa fragment. The smaller fragment corresponds to S5-P (open triangle) and the presence of a 36-kDa fragment suggests that T1 was partially digested (solid triangle; diagrammed in the cartoon in Figure 11C). Taken together, these findings imply the following. T1 inhibits the activity of some, but not all, signal sequences; a folded T1 structure may underlie inhibition of signal sequence activity (see Discussion).

DISCUSSION

Topogenic determinants encoded within Kv1.3 direct a topology that is consistent with that reported by Shih and Goldin (*3*) for the *Shaker* K^+ channel. However, how this final topology is achieved during biogenesis in the endoplasmic reticulum is not known. The combination of protease protection assays and carbonate extraction assays indicates that five transmembrane segments (S1, S2, S3, S5, and S6) initiate translocation (have signal sequence activity). S1 and S2 function as a signal anchors and efficiently integrate into the membrane, whereas S4 and S5 show weaker integration. S3 and S6 alone lack the ability to integrate into the membrane.

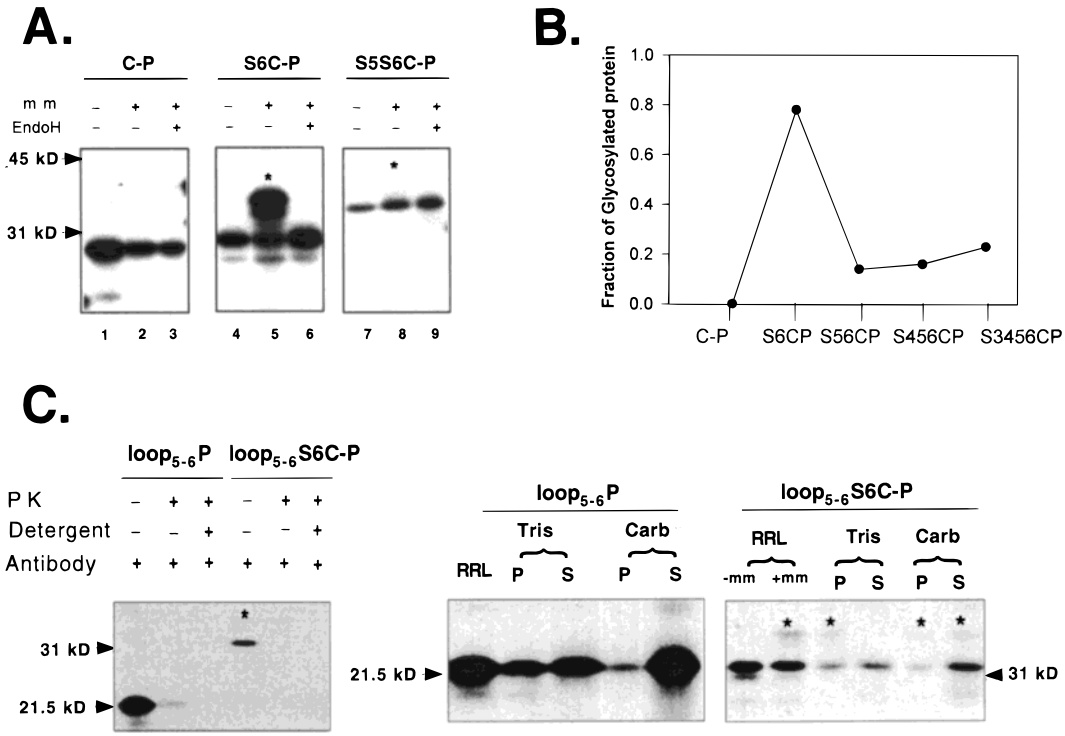

FIGURE 9: Modulation of the C-terminus of Kv1.3 topology by covalently linked N-terminal additions. (A) For the constructs C-P, S6C-P, and S5-S6C-P, protein was translated in the presence or absence of microsomal membranes and in the presence or absence of endoglycosidase. The bands directly below the asterisk in lanes 5 and 8 are due to glycosylated protein. (B) Fraction of protein glycosylated was calculated for each construct, plus results for S4-S5-S6C-P and S3-S4-S5-S6C-P (gels not shown), and plotted as a function of increasing number of transmembrane segments. All constructs except C-P and S6C-P are integrated and minimally glycosylated, i.e., their C-termini are in the cytosol. (C) Protease protection and carbonate extraction of $loop_{5,6}$-P and $loop_{5,6}$-S6C-P. Microsomal membranes containing translated $loop_{5,6}$-P and $loop_{5,6}$-S6C-P were treated as described in Figure 1 and analyzed by SDS−PAGE (left panel) or extracted into either Tris buffer (pH 7.5) or carbonate buffer (pH 11.5) and processed as described in Figure 2 to determine pellet−supernatant distributions of the protein (right panel). The observed molecular masses for unglycosylated constructs are ∼21 and ∼32 kDa, respectively, for $loop_{5,6}$-P and $loop_{5,6}$-S6C-P. In the case of $loop_{5,6}$-S6C-P, the construct was translated in the absence (−mm) and presence (+mm) of microsomal membranes, the latter producing an additional weak band (<10%) at ∼35 kDa that was glycosylated protein. This was confirmed by endoglycosidase digestion (data not shown). A single asterisk marks a band due to glycosylated protein. Protease protection for $loop_{5,6}$ and $loop_{5,6}$-S6C-P was 8% and 12%, respectively. Integration was 12% and 11%, respectively.

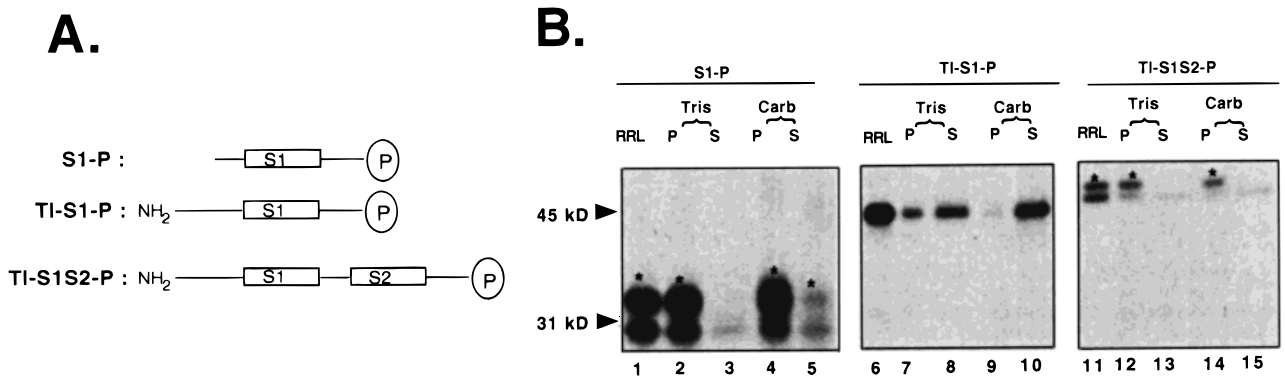

FIGURE 10: Modulation of S1-P topology by covalently linked amino terminus (T1). (A) Schematic diagram of S1-P, T1-S1-P, and T1-S1-S2-P. (B) Translation products for the constructs shown in panel A were extracted into either Tris buffer (pH 7.5) or carbonate buffer (pH 11.5), centrifuged to give pellet (P) and supernatant (S) fractions, and analyzed by SDS−PAGE as described in Figure 2. Lanes 2−5 show the distribution of S1-P. Two bands were detected, the lower is the unglycosylated S1-P and the upper band (*) is the glycosylated S1-P. S1-P is integrated into the membrane and is found in the pellets following either Tris or carbonate extraction. Lanes 7−10 show the distribution of T1-S1-P. It is preferentially located in the supernatants following extraction with either buffer. It displays no glycosylated bands. Lanes 12−15 show the distribution of T1-S1-S2-P. It behaves just like S1-P, preferentially integrated into the membrane, and glycosylated (*).

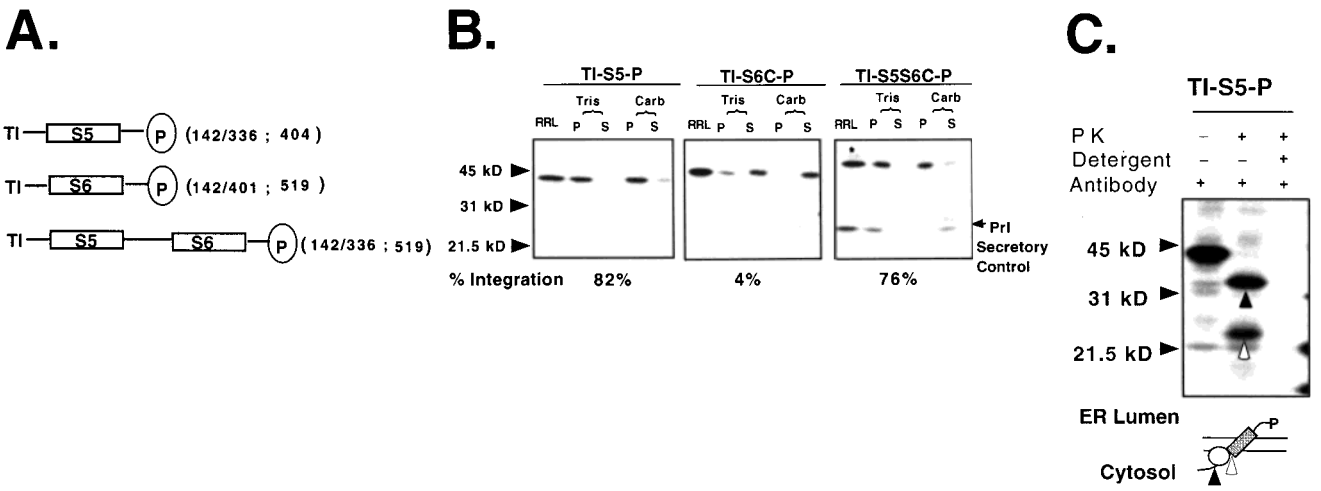

FIGURE 11: Modulation of S5 and S6 membrane integration by covalently linked T1. (A) Schematic of P-reporter constructs containing T1. The numbers in parentheses are the amino acid numbers in the native sequence that encode the linked amino acids and P-reporter sites, written as (last T1 amino acid/first amino acid of the transmembrane segment; amino acid where P-reporter is inserted). (B) For constructs T1-S5-P, T1-S6C-P, and T1-S5-S6-P, translation products were each extracted into either Tris buffer (pH 7.5) or carbonate buffer (pH 11.5) and processed as described in Figure 2 to determine pellet−supernatant distributions of the protein. The predicted molecular masses for unglycosylated constructs are 39, 44, and 51 kDa, respectively. Prl was included as a secretory control to demonstrate the integrity of the membranes. Filled, sideways arrowheads mark control protein bands, Prl, and the positions of molecular weight standards. A single asterisk marks a band due to glycosylated protein. The percent integration, calculated as described under Materials and Methods, is given below the gel for each construct. (C) Protease protection of T1-S5-P. Microsomal membranes containing translated T1-S5-P were treated as described in Figure 1 and analyzed by SDS−PAGE. A cartoon representation of T1-S5-P topology is indicated below the gel. The solid and open triangles represent proteolytic cleavage sites, the latter one corresponding to the cryptic cleavage site in S5-P (Figures 1 and 2). The P-protected fragments in the gel are correspondingly labeled.

Surprisingly, approximately 51% of the S4 pool integrated into the membrane despite the fact that S4 is a highly charged peptide containing seven basic residues, distributed every third amino acid. Thus, if S4 is a standard α-helix with 3.6 residues per turn, then these charges do not all align on one face of the helix. Some may face the cytosol or interact with negative phospholipid headgroups or span the bilayer. Regardless, the C-terminus of S4 would be in the cytosol. Structural and topological experiments have been carried out by Peled-Zehavi et al. (*30*) using optical techniques to study synthetically made S3 and S4 *Shaker* segments. These workers have shown that S3 and S4 have partially α-helical structure in a hydrophobic environment and each interacts strongly with phospholipid membranes. Moreover, the S4 peptide orients parallel to the membrane surface, consistent with our data, while S3 tends to be transmembrane, which differs from our results. This discrepancy may be due to several differences between our S3-P Kv1.3 construct and the synthetic S3 *Shaker* peptide used in the spectroscopic studies of Peled-Zehavi et al. (*30*). The latter contains an extended N-terminus, including more of the S2-S3 *Shaker* loop. The amino acids in the regions flanking the hydrophobic S3 of *Shaker* are different from those in Kv1.3, including differences in charged residues, which can significantly alter the topology of transmembrane segments (*22*).

Although S4 itself can integrate into the membrane, it does not translocate its C-terminus flanking region: the P-reporter in S4-P is almost completely (95%) digested by PK. However, the inability of S4 to translocate its C-terminus can be modulated. For instance, the P-reporter in S3-S4-P

and S2-S3-S4-P are protected 25% and 17%, respectively, indicating that S4 does get translocated when it is included in a polytopic protein. Translocation of highly charged peptide sequences do occur, the most notable examples being cleavable signal sequences of imported mitochondrial proteins (*31*). This presumably occurs through a water-filled translocon channel.

The impact of additional transmembrane segments is manifest in both the kinetics and steady-state levels of integration and translocation of the protein. If each transmembrane segment were an α-helix that independently inserted into the membrane, then each would contribute ~30 kcal/mol of stabilization due to hydrophobic interactions of each helix with the membrane (*32*). A protein containing multiple, and potentially interactive, transmembrane segments is more complicated and it is not yet possible to predict the consequent energetics of membrane insertion.

Nonetheless, we can infer potential interactions between transmembrane segments. For example, one candidate interaction unit is S2-S3-S4. The ability of S5 to translocate its C-terminus is impaired by the presence of S4 and S3 and can be restored if S2 is additionally present. Maximum protection of the P-reporter decreased to 29% and 20%, respectively, for S4-S5-P and S3-S4-S5-P. In contrast, the P-reporter in S2-S3-S4-S5-P was protected 48%. Although interactions between transmembrane segments during biogenesis can be direct or indirect, protein−protein interactions between transmembrane segments have been implicated in the gating of Kv channels (e.g., refs *33*−*37*). Peled-Zehavi et al. (*30*) have shown in artificial membranes that neither S3 nor S4 segments can self-associate, but they associate with the S2 segment and with each other. It is possible that such modular units are first manifest as interacting transmembrane domains during assembly that help direct topogenesis, thereby ensuring the requisite structure for their subsequent role as functional units in the channel.

Another candidate interaction unit, S5-S6C, is implicated by the finding that C-terminus topology of Kv1.3 is already manifest in S5-S6C-P. The pore loop and $loop_{5,6}$-S6C-P do not have signal sequence activity. The additional presence of S5 is required for integration and correct topology. These results suggest that S5, S6-C-terminus, and/or the pore loop may associate in the translocon of the microsomal membrane to establish correct topology. The crystal structure of KcsA channel reveals a close proximity of the pore helix and the transmembrane segment corresponding to S6 (*1*). Such an interaction could alter translocation activity of S6, confining the C-terminus to the cytosol. Additionally, S5−S6 may interact to form the tertiary channel structure during translation of the protein monomer and also to facilitate insertion of the S6 into the bilayer. These combined interactions could thus establish the topology of Kv channels. In this model, two purposes, one functional, one architectural, would be served by the same amino acid sequences.

Dual-purpose transmembrane sequences have precedent in other multisubunit protein complexes. For example, a conserved 20 amino acid sequence in hydrophobic membrane proteins of periplasmic permeases plays a critical role in intersubunit association interactions and also participates in formation of a functional site for transport activity (*38*). Another example of the same transmembrane sequence bearing information for assembly and for ER retention/degradation is the T-cell receptor α-subunit/CD3-δ (*39*). A similar mechanism may occur in assembly of the SUR−KIR channel (*40*). We would like to suggest that association sites between transmembrane segments modify topogenic and functional determinants, perhaps via the same intramembrane protein−protein interaction.

Another intriguing finding in this study is the observation that the N-terminus of Kv1.3 influences transmembrane topology of some segments. S1 translocates and integrates into the bilayer, T1-S1 does neither, yet T1-S1-S2 translocates the C-terminus of S1 and integrates very efficiently. Thus, S2 likely functions as the initial signal sequence to establish Kv1.3 N-terminus topology. This is similar to findings reported for CFTR (*6*) in which the second transmembrane segment directs protein topology. One speculation for why S2, rather than S1, initiates translocation is that nascent T1 and S1 would stay in the cytosol for a longer time, thereby promoting interactions required for efficient T1 recognition function. Although the mechanism by which T1 blocks signal sequence activity of S1 is unknown, one or more of the following possibilities may be responsible. First, T1 may itself inhibit signal sequence activity; it may even form a folded structure or interact with another T1 to form a highly ordered structure (*25*, *26*, *41*) that inhibits signal sequence activity. Second, T1 may interact with residues in region C of the N-terminus to inhibit signal sequence activity. Third, T1 may nonspecifically inhibit signal sequence activity. The results of PK digestion and carbonate extraction assays for T1-S5-P suggest that T1 does not inhibit targeting of S5-P to the membrane but rather a later translocation event. Moreover, Denzer et al. (*42*) have shown that the folding behavior, rather than the length, of N-terminal domains of integrated membrane proteins is the determining factor in their topogenesis. Stable folding of these domains hindered or even prevented N-terminal translocation, although the proteins were targeted correctly and integrated into the ER membrane. There is evidence that the N-terminus of some Kv proteins is associated in a highly ordered structure (*41*) and can exist as a folded complex with Zn ions (*43*). Although these Kv precedents involve interas well as intrasubunit interactions, they nonetheless indicate a tendency for T1 to form folded structures.

The second possible cause of inhibition of signal sequence activity in T1-S1-P is that T1 interacts with other parts of Kv1.3, namely, the C region of S1-P. As defined by Shen and Pfaffinger (*28*), the N-terminus of Kv channels is composed of three consecutive regions: A, B, and C. The latter was included as the N-terminus of the S1-P construct. The mere presence of the C region of the N-terminus in T1-S1-P cannot be responsible for inhibition of T1-S1 translocation and integration because S1-P, which contains only the C region, can translocate S1 and integrate efficiently. We hypothesize that regions A, B, and C together may form a structural unit that leads to a conformation in which S1 signal sequence activity is blocked. Such a structure has been reported for a *Shaw* channel, in which a protein layer just under the inner face of the membrane (perhaps region C) is involved in an intersubunit Zn-binding complex (*43*). Although Kv1.3 is a member of the *Shaker* family, it resembles the *Shaw* Kv3.1, and not *Shaker*, with respect to cysteine motifs in the N-terminus that are involved in the *Shaw* Kv3.1 Zn-binding complex.

In addition to mechanisms of channel biogenesis, these studies have some bearing on the mechanisms whereby peptide fragments made from the central core of Kv1.3 suppress current when coexpressed with Kv1.3 (*11*). T1-S1 potently and specifically suppresses Kv1.3 channel expression (*29*). T1-S1 does not integrate into the membrane. The mechanism by which T1-S1 suppresses channel assembly may include inhibition of translation, translocation, and/or integration, any of which could occur if T1-S1 associates with nascent channel protein while it is being translated. Alternatively, T1-S1 could inhibit assembly by competing for cytosolic intersubunit interactions involved in dimer or tetramer formation (*44*). We now speculate that the mechanism of T1-S1 suppression is fundamentally different from that involved in suppression caused by peptide fragments derived from the central core of Kv1.3 including portions of S1 through S6 (*11*). The latter requires protein−protein association within the bilayer (*12*); the former does not. Some fragments from the central core of Kv1.3 are strong suppressors (e.g., S1-S2-S3 and S3-S4-S5; *11*) and integrate into the membrane (*12*; this paper). If correct orientation alone of membrane-integrated Kv1.3 fragments were sufficient to cause suppression by a nonspecific mechanism, then S5-S6COOH and S1 should be strong suppressors. However, they are not (*11*). Together, these results suggest that the ability of core peptide fragments of Kv1.3 coexpressed with Kv1.3 to suppress current may reflect specific association sites.

ACKNOWLEDGMENT

We thank Dr. Richard Horn for reading the manuscript.

REFERENCES

1. Doyle, D. A., Cabral, J. M., Pfuetzner, R. A., Kuo, A., Gulbis, J. M., Cohen, S. L., Chait, B. T., and MacKinnon, R. (1998) *Science 280*, 69−77.
2. Perozo et al. (1998) *Nat. Struct. Biol. 5*, 459−469.
3. Shih, T. M., and Goldin, A. L. (1997) *J. Cell Biol. 136*, 1037−1045.
4. Braell, W. A., and Lodish, H. F. (1982) *Cell 28*, 23−31.
5. Shi, L.-B., Skach, W. R., Ma, T., and Verkman, A. (1995) *Biochemistry 34*, 8250−8256.
6. Lu, Y., Xiong, X., Helm, A., Kimani, K., Bragin, A., and Skach, W. R. (1998) *J. Biol. Chem. 273*, 568−576.
7. Calamia, J., and Manoil, C. (1992) *J. Mol. Biol. 224*, 539−543.
8. Skach, W. R., and Lingappa, V. (1993) *J. Biol. Chem. 268*, 23552−23561.
9. Moss, K., Helm, A. Lu, Y., Bragin, A., and Skach, W. R. (1998) *Mol. Biol. Cell 9*, 2681−2697.
10. Wilkinson, B., Critchley, A., and Stirling, C. (1996) *J. Biol. Chem. 271*, 25590−25597.
11. Tu, L., Santarelli, V., Sheng, Z.-F., Skach, W., Pain, D., and Deutsch, C. (1996) *J. Biol. Chem.* 271, 18904−18911.
12. Sheng, Z., W. Skach, V. Santarelli, and C. Deutsch. (1997) *Biochemistry 36*, 15501−15513.
13. Skach and Lingappa (1993) in *Mechanisms of Intracellular Trafficking and Processing of Proproteins*. (Loh, P., Ed.) pp 19−77, CRC Press, Boca Raton, FL.
14. Fujiki, Y., Hubbard, A. L., Fowler, S., and Lazarow, P. (1982) *J. Cell Biol. 93*, 97−102.
15. Chahine, M., Chen, L., Barchi, R. L., Kallen, R. G., and Horn, R. (1992) *J. Mol. Cell. Cardiol. 24*, 1231−1236.
16. Rothman, R. E., Andrews, D. W., Calayag, M. C., and Lingappa, V. (1988) *J. Biol. Chem. 263*, 10470−10480.
17. Aberijon, C., and Hirschberg, C. B. (1990) *J. Biol. Chem. 265*, 14691−14695.
18. Friedlander, M., and Blobel, G. (1985) *Nature 318*, 338−343.
19. Audigier, Y., Friedlander, M., and Blobel, G. (1987) *Proc. Natl. Acad. U.S.A. Sci. 84*, 5783−5787.
20. Skach, W. R., Shi, L., Calayag, M. C., Frigeri, A., Lingappa, V. R., and Verkman, A. S. (1994) *J. Cell Biol. 125*, 803−815.19.
21. Lipp, J., and Dobberstein, B. (1986) *Cell 46*, 1103−1112.
22. Schmid, S. R., and Speiss, M. (1988) *J. Biol. Chem. 163*, 16886−16891.
23. Nothwehr, S. F., and Gordon, J. I. (1990) *J. Biol. Chem. 265*, 17202−17208.
24. Hartmann, E., Rapoport, T. A., and Lodish, H. F. (1989) *Proc. Natl. Acad. Sci. U.S.A. 86*, 5786−5790.
25. Li, M., Jan, Y. N., and Jan, L. Y. (1992) *Science 257*, 1225−1230.
26. Shen, N. V., Chen, X., Boyer, M. M., and Pfaffinger, P. (1993) *Neuron 11*, 67−76.
27. Xu, J., Yu, W., Jan, Y. N., Jan, L. Y., and Li, M. (1995) *J. Biol. Chem. 270*, 24761−24768.
28. Shen, N. V., and Pfaffinger, P. (1995) *Neuron 14*, 625−633.
29. Tu, L., Santarelli, V., and Deutsch, C. (1995) *Biophys. J. 68*, 147−156.
30. Peled-Zehavi, H., Arkin, I. T., Engelman, D. M., and Shai, Y. (1996) *Biochemistry 35*, 6828−6838.
31. von Heijne, G. (1988) *Biochim. Biophys. Acta 947*, 307−333.
32. Lemmon, M. A., and Engelman, D. M. (1994) *Q. Rev. Biophys. 27*, 157−218.
33. Papazian, D. M., Shao, X. M., Seoh, S.-A., Mock, A. F., Huang, Y., and Wainstock, D. H. (1995) *Neuron 14*, 1293−1301.
34. Planells-Cases, R., Ferrer-Monteil, A. V., Patten, C. D., and Montal, M. (1995) *Proc. Natl. Acad. Sci. U.S.A. 92*, 9422−9426.
35. Seoh, S. A., Sigg, D., Papazian, D. M., and Bezanilla, F. (1996) *Neuron 16*, 1159−1167.
36. Tiwari-Woodruff, S. K., Schulteis, C. T., Mock, A. F., and Papazian, D. M. (1997) *Biophys. J.* 72, 1489−1500.
37. Monks, S. A., Needleman, D. J., and Miller, C. (1999) *J. Gen. Physiol. 113*, 415−423.
38. Mourez, M. H., Hofnung, M., and Dassa, H. (1997) *EMBO J. 16*, 3066−3077.
39. Bonifacino, J. S., Cosson, P., and Klausner, R. D. (1990) *Cell 63*, 503−513.
40. Zerangue, N., Schwappach, B., Jan, Y. N., and Jan, L. Y. (1999) *Neuron 22*, 537−548.
41. Kreusch, A., Pfaffinger, P. J., Stevens, C. F., and Choe, S. (1998) *Nature 392*, 945−948.
42. Denzer, A. J., Nabholz, and Speiss, M. (1995) *EMBO J. 14*, 6311−6317.
43. Bixby, K. A., Nanao, M. H., Shen, N. V., Kreusch, A., Bellamy, H., Pfaffinger, P. J., and Choe, S. (1999) *Nat. Struct. Biol. 6*, 38−43.
44. Tu, L., and Deutsch, C. (1999) *Biophys. J. 76*, 2004−2017.

BI991740R